ELSEVIER

Journal of Molecular Structure 446 (1998) 15–39

Journal of
MOLECULAR
STRUCTURE

Raman and infrared spectra, conformational stability, ab initio calculations and vibrational assignments for chloromethyl methyl silane

Gamil A. Guirgis, Yasser E. Nashed, James B. Robb II, James R. Durig*

Department of Chemistry, University of Missouri—Kansas City, Kansas City, MO 64110-2499 USA

Received 28 July 1997; accepted 1 September 1997

Abstract

The infrared (3500 to 30 cm^{-1}) spectra of gaseous and solid and the Raman (3500 to 10 cm^{-1}) spectra of the liquid with quantitative depolarization ratios and solid chloromethyl methyl silane, $ClCH_2SiH_2CH_3$, have been recorded. Similar data have also been recorded for the Si-d_2 isotopomer. These data indicate that two conformers are present in the fluid states but only one conformer is present in the annealed crystalline state. The mid-infrared spectra of the sample dissolved in liquified xenon as a function of temperature (− 100 to − 70°C) have been recorded. Utilizing conformer pairs at 738 (*gauche*), 685 (*gauche*), and 700 (*trans*) cm^{-1} the enthalpy difference has been determined to be 180 ± 18 cm^{-1} (515 ± 51 cal mol^{-1}) with the *gauche* conformer the more stable species. However, in the spectrum of the solid, the *trans* conformer is the stable rotamer remaining after the sample is well annealed. Utilizing the Si–H stretching frequencies from the infrared spectrum of the $ClCH_2SiHDCH_3$ isotopomer, the two Si–H bond distances are calculated to be 1.482 and 1.487 Å for the *gauche* conformer. The optimized geometries, conformational stabilities, harmonic force fields, infrared intensities, Raman activities, depolarization ratios, and vibrational frequencies are reported for both conformers from RHF/6-31G* and/or MP2/6-31G* ab initio calculations. The *gauche* conformer is predicted to be the more stable rotamer from both ab initio calculations in agreement with the experimental results. The other calculated quantities are compared to the experimentally determined values where applicable as well as with some corresponding results for some similar molecules. © 1998 Elsevier Science B.V.

Keywords: Chloromethyl methyl silane; Conformational stability; Ab initio calculations; Raman and infrared spectra

1. Introduction

Previously we [1] investigated the far infrared and low frequency gas phase Raman spectra of the 1-halopropane molecules, $CH_3CH_2CH_2X$ where X = F, Cl and Br, and from the observed asymmetric torsional transitions of both the *trans* and *gauche* conformers the potential functions governing the conformer interconversions were determined. From these potential functions the enthalpy differences between the high energy *trans* and the low energy *gauche* conformers were estimated. The values ranged from 127 ± 10 cm^{-1} for the chloride, 122 ± 10 cm^{-1} for the fluoride, and 35 ± 10 cm^{-1} for the bromide. However, the experimental determined values had such large uncertainties (i.e. for the chloride [2–4] ~0, − 5 ± 10, 17 ± 52 cm^{-1}; for the fluoride [5] 164 ± 108; and for the bromide [4] 35 ± 70 cm^{-1}) that it was not

* Corresponding author.

0022-2860/98/$19.00 © 1998 Elsevier Science B.V. All rights reserved
PII S0022-2860(97)00346-3

possible to make meaningful comparison with the estimated values. Nevertheless, the experimental results indicated that the *gauche* conformers are the more stable rotamers in the gas phase but for the chloride, bromide and iodide the *trans* conformer is the more stable form in the crystalline solid [3]. In contrast, for the fluoride the *gauche* conformer appears to be the more stable rotamer in all physical states [6].

For the corresponding chlorosilane, $ClCH_2SiH_2CH_3$, the stable conformer in the crystalline state is the *trans* form but in the liquid state it was estimated that the enthalpy difference was zero between the two conformers [7]. In the vapor state the infrared bands of the conformer pairs are so badly overlapped that measurements of the relative intensities of the bands were not possible [7]. Therefore, to determine the conformer stability in the fluid states we have carried out a temperature dependent infrared spectral investigation of chloromethyl methyl silane dissolved in liquid xenon. Since the Raman spectra had not been reported in the previous vibrational study [7] we have recorded Raman data for both the liquid and solid. As an aid in interpreting the vibrational spectra we have carried out ab initio calculations at the RHF/3-21G*, RHF/6-31G* and MP2/6-31G* levels. The optimized geometries, conformational stabilities, harmonic force fields, infrared intensities, Raman activities, depolarization ratios, and vibrational frequencies have been obtained to compare with the experimental results where applicable. The results of these spectroscopic and theoretical studies are reported herein.

2. Experimental

The samples of chloromethyl methyl silane and the deuterated species Si-d_2 were prepared by the reduction of commercially available chloromethyl methyl dichlorosilane with lithium aluminum hydride -d_0 and -d_4 in dry dibutyl ether. Purification was performed with a low-temperature, low-pressure fractionating column, and the purity of the sample was checked by recording the mass spectrum and the mid-infrared spectrum of the gas. The sample was stored under vacuum at low temperature.

The Raman spectra were recorded on a SPEX model 1403 spectrophotometer equipped with a Spectra-Physics model 164 argon ion laser operating on the 514.5 nm line. The laser power used was 0.5 W for the liquid and the solid with slit widths of 3 cm^{-1}. The spectra of the liquids were recorded with the samples sealed in a Pyrex glass capillary contained in capillary tubes held in a Miller–Harney apparatus [8]. The Raman spectra of the solids were obtained by cooling the liquids until the samples solidified.

Depolarization measurements were obtained for the liquid samples using a standard Ednalite 35 mm camera polarizer with 38 mm of free aperture affixed to the SPEX instrument. Depolarization ratio measurements were checked by measuring the state of polarization of the Raman bands of CCl_4 immediately before depolarization measurements were made on the liquid sample. The measurements of Raman frequencies are expected to be accurate to $\pm$ 2 cm^{-1} and typical spectra are shown in Figs. 1 and 2.

The mid-infrared spectra (Figs. 3 and 4) of the gases and solids were recorded using a Perkin-Elmer model 2000 Fourier transform interferometer equipped with a Ge/CsI beamsplitter and DTGS detector. Atmospheric water vapor was removed from the spectrometer housing by purging with dry nitrogen. The spectra of the gas were obtained by using a 10 cm cell fitted with CsI windows. The spectra of the solids were obtained by condensing the sample on a CsI substrate held at the temperature of boiling liquid nitrogen, housed in a vacuum cell fitted with CsI windows. The samples were condensed as amorphous or glassy solids and repeatedly annealed until no further changes were observed in the spectra.

The mid-infrared spectra of the sample dissolved in liquified xenon as a function of temperature were recorded on a Bruker model IFS 66 Fourier transform interferometer equipped with a globar source, a Ge/KBr beamsplitter and a TGS detector. In all cases 100 interferograms were collected at 1.0 cm^{-1} resolution, averaged and transformed with a boxcar truncation function. For these studies a specially designed cryostat cell was used. It consisted of a copper cell with a path length of 4 cm with wedged silicon windows sealed to the cell with indium gaskets. It was cooled by boiling liquid nitrogen to 77 K. The temperature was monitored with two Pt thermoresistors. The complete cell was connected to a pressure manifold, allowing the filling and evacuation of the cell. After

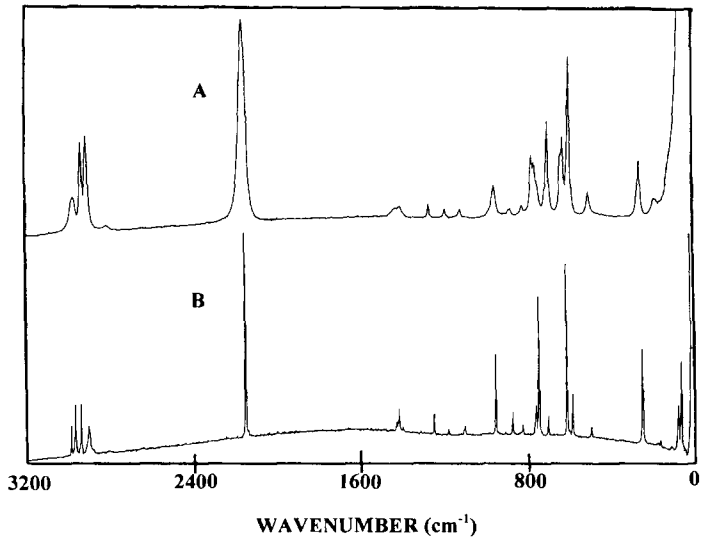

Fig. 1. Raman spectra of chloromethyl methyl silane-d_0: (A) liquid; and (B) annealed solid.

the cell had cooled to the desired temperature, a small amount of the compound was condensed into the cell. Next, the pressure manifold and the cell were pressurized with the noble gas, which immediately started to condense in the cell, allowing the compounds to dissolve.

The far infrared spectra (Figs. 5 and 6) of gaseous chloromethyl methyl silane and the Si-d_2 compound were recorded on a Bomen model DA3.002 Fourier transform interferometer equipped with a vacuum bench, using 6.25 and 25 μm Mylar beamsplitters, and a liquid helium-cooled Si bolometer. The spectra were obtained from the samples contained in a 1 m folded path cell equipped with mirrors coated with gold, and fitted with polyethylene windows with an effective resolution of 0.10 cm^{-1}. To remove traces of

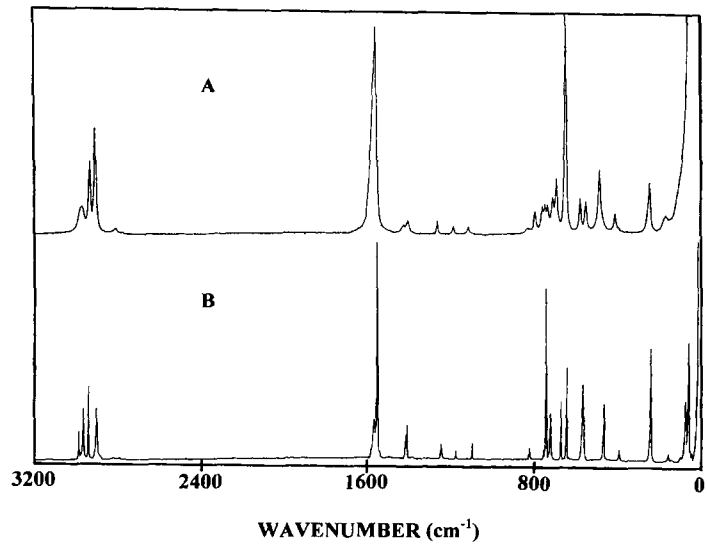

Fig. 2. Raman spectra of chloromethyl methyl silane-d_2: (A) liquid; and (B) annealed solid.

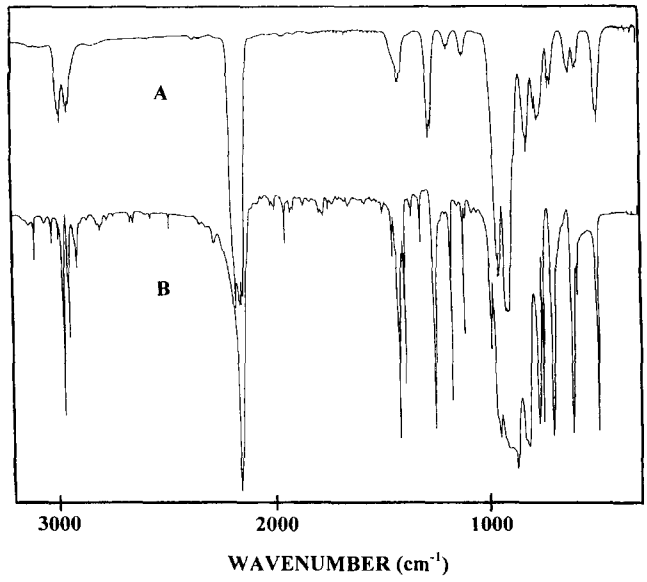

Fig. 3. Mid-infrared spectra of chloromethyl methyl silane-d_0: (A) gas; and (B) annealed solid.

water, an activated 4 Å molecular sieve was used to dry the sample. The spectra of the amorphous and crystalline solids were obtained with the Perkin-Elmer model 2000 equipped with a metal grid beam-splitter and a DTGS detector. All of the observed bands with their proposed assignments are listed in Tables 1 and 2.

3. Conformational stability

The determination of the conformational stability is not straight forward since most of the fundamentals for each conformer are predicted to be near coincident. Nevertheless, it is quite clear from the spectral data that conformers are present in the fluid phases.

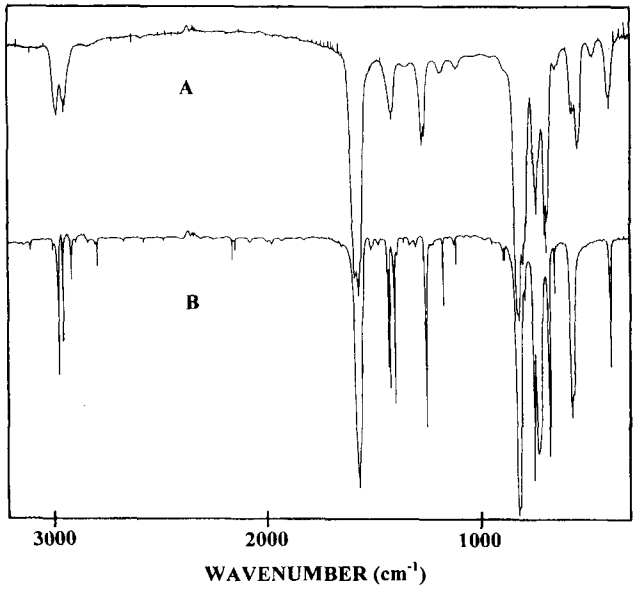

Fig. 4. Mid-infrared spectra of chloromethyl methyl silane-d_2: (A) gas; and (B) annealed solid.

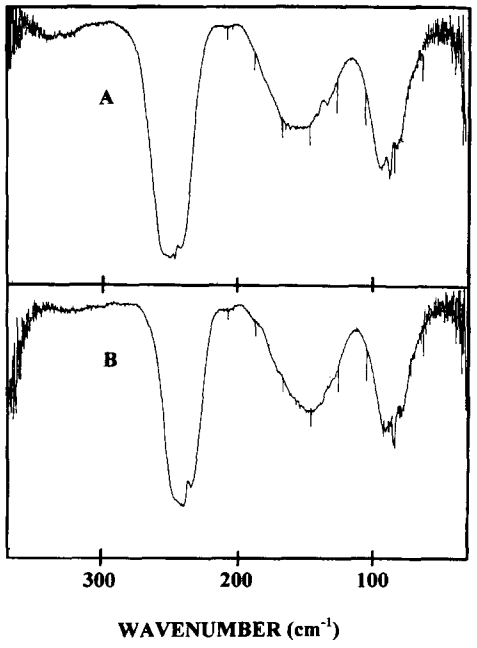

Fig. 5. Far infrared spectra of chloromethyl methyl silane gas: (A) -d_0; and (B) -d_2.

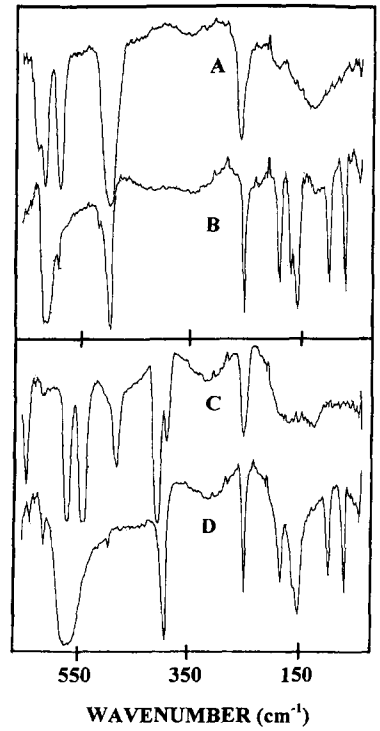

Fig. 6. Far infrared spectra of chloromethyl methyl silane: (A) unannealed solid-d_0; (B) annealed solid-d_0; (C) unannealed-d_2; and (D) annealed-d_2.

For example, a comparison of the Raman spectrum of the liquid to that of the solid clearly shows that several bands disappear with solidification of the sample. Pronounced Raman lines at 623 and 688 cm^{-1} in the spectrum of the liquid are absent from the spectrum of the solid. Similarly infrared bands at 685 (pronounced Q-branch) and 624 cm^{-1} (maximum in the spectrum of the gas which are found at 685 and 619 cm^{-1} in the spectrum of the amorphous solid) are absent from the spectrum of the solid. Similarly there are bands at 738 and 580 cm^{-1} which also disappear from the spectrum of the amorphous sample when the sample is annealed to a polycrystalline solid (Fig. 1). Therefore, in both the spectra of the gas and liquid there is clear evidence for the existence of two conformers. The ab initio calculations indicate that the bands which disappear are due to the *gauche* conformer so the *trans* conformer is the rotamer that is stable in the solid.

The conformer pairs at 685/700 and 738/700 cm^{-1} with the first listed frequency due to the *gauche* conformer were used to determine the enthalpy difference between the conformers by the temperature dependent infrared spectra of xenon solutions of the normal species. The spectral changes are shown in Fig. 7 for the first pair of bands and from these spectral data, it is obvious that the increase in the intensity of the infrared band assigned to the *gauche* conformer as the temperature decreases confirmed the stability of the *gauche* rotamer over the *trans* conformer in the xenon solution. In order to obtain the enthalpy difference, seven spectral data points were obtained for these lines over the temperature range −70 to −100°C (Table 3). The intensities of each conformer pair were fit to the equation $-\ln K = (\Delta H/RT) - (\Delta S/R)$ where K is the intensity ratio (I_g/I_t), and it is assumed that ΔH is not a function of temperature. Using a least squares fit, and from the slope of the line (Fig. 8), a ΔH value of 181 ± 6 cm^{-1} [518 ± 17 cal mol^{-1} (1 cal = 4.184 J)] was obtained from the lower wavenumber conformer pair and a value of 180 ± 5 cm^{-1} (515 ± 14 cal mol^{-1}) obtained from the pair at 738/700 cm^{-1}. The average value from these two determinations is 180 ± 18 cm^{-1} (343 ± 51 cal mol^{-1}). This value should be near the value for the gas [9,10] since

Table 1
Observed infrared[a] and Raman wavenumbers (cm^{-1}) for chloromethyl methyl silane-d_0

Infrared						Raman				Assignment	
Gas	Rel. int.	Solid	Rel. int.	Xenon gas	Rel. int.	Liquid	Rel. int. & Depol.	Solid	Rel. int.	ν_i^b	Approximate Description
3107 R											
3085 Q,A	vw	3099	w								
3069 P											
		3019	w								
2990 R											
2987 Q	m	2990	w	2975	m	2976	w,dp	2992	w	ν_1,ν_{17}	CH_3 antisymmetric stretch
2984 Q	m									ν_{18}'	CH_2 antisymmetric stretch
2977 Q	m	2968	vs	2970	m			2973	w	ν_{18}	CH_2 antisymmetric stretch
2974 P											
2949 R											
2944 Q	m	2947	w							ν_2'	CH_2 symmetric stretch
2940 Q	m	2943	s	2934	m	2940	m,p	2946	w	ν_2	CH_2 symmetric stretch
2937 P											
		2915	sh								
2917	sh,w	2906	w	2913	w	2915	m,p	2910	w	ν_3,ν_3'	CH_3 symmetric stretch
								2890	sh		
2832	vw					2817	vw,p				
2179 R											
2174 Q,C	vs	2160	vs	2167	vs	2162	vs,p	2157	vs	ν_{19}	SiH_2 antisymmetric stretch
2172 Q,C	vs									ν_{19}'	SiH_2 antisymmetric stretch
2154 R											
2148 Q,A	vs	2151	sh,vs	2144	vs	2162	vs,p	2157	vs	ν_4	SiH_2 symmetric stretch
2146 Q,A	vs									ν_4'	SiH_2 symmetric stretch
2141 P											
		1443	m								
1430 bd	m	1431	m	1433	w	1424	w,dp	1427	w	ν_{20}	CH_3 antisymmetric deformation
		1422	s	1424	sh					ν_{20}'	CH_3 antisymmetric deformation
		1416	vs					1416	w	ν_5	CH_3 antisymmetric deformation
		1410	m	1417	m					ν_5'	CH_3 antisymmetric deformation
		1400	m	1408	w						
1410 R											
1402 Q	m	1388	s	1395	m	1402	w,dp	1406	w	$\nu 6$	CH2 deformation
1396 P				1384	w						
		1350	w								
		1310	m								
1268 R											
1262 ctr,B	m	1250	vs	1256	s	1259	w,p	1248	m	ν_7	CH_3 symmetric deformation
1257 P	1234	sh,m									

1184 R											
1179 Q,A	w	1171	vs	1176	m	1181	w,p	1180	w	ν_8	CH_2 wag
1174 P		1167	sh,m								
1113 R											
1108 Q,A	w	1111	s	1104	m	1110	w,dp	1099	w	ν_{21}	CH_2 rock
1102 P											
		988	s								
953 R											
948 Q,A	vs	948	vs			944	m,dp	954	s	ν_9	SiH_2 deformation
947 Q,A	vs			942	vs	944	m,dp			ν_9'	SiH_2 deformation
941 P											
914 R											
906 Q,A	vs	905	vs	898	vs	910	vvw			ν_{10}	SiH_2 wag
898 P											
				888	vs					ν_{10}'	SiH_2 wag
				871	s			874	w	ν_{22}	CH_3 rock
869 Q	s	870	vs	865	s	871	w,dp			ν_{22}'	CH_3 rock
818 R				820	sh			824	w	ν_{23}	CH_3 twist
812 Q,C	m	815	vs	810	s	811	w,p			ν_{23}'	CH_3 twist
773	m	768	s	764	s	765	m,p	762	w	ν_{11}	C–Cl stretch
760 R											
754 ctr,B	m	746	s	749	sh	752	m,p	748	m	ν_{12}	CH_3 rock
747 P				738	m					ν_{12}'	CH_3 rock
707 R											
702 Q,A	m	703	s	700	m	700	sh,p	702	w	ν_{13}	C_1–Si stretch
696 P											
658 Q,C	w			685	w	688	m,p			ν_{13}'	C_1–Si stretch
624	R										
615 Q	w			618	w	623	m,p			ν_{14}'	Si–C_3 stretch
611 Q	w	611	s	608	w	613	m,p	614	s	ν_{14}	Si–C_3 stretch
606 P											
588 R											
581 Q	w	584	s					586	m	ν_{24}	SiH_2 twist
580 Q				581	m	584	s,p			ν_{24}'	SiH_2 twist
575 P											
493 R											
486 Q,C	m			488	s	492	w,p			ν_{25}'	SiH_2 rock
479 P											

Table 1
(*continued*)

Infrared						Raman				Assignment	
Gas	Rel. int.	Solid	Rel. int.	Xenon gas	Rel. int.	Liquid	Rel. int. & Depol.	Solid	Rel. int.	ν_i^b	Approximate Description
470 Q	w	492	s	473	sh			497	w	ν_{25}	SiH_2 rock
		249	s			255	sh,m	253	m	ν_{15}	SiC_3Cl bend
249 R											
246 Q,C	s					246	m,p			ν_{15}'	SiC_3Cl bend
242 P											
160 Q,sh	w					168	vw			ν_{26}'	CH_3 torsion
154 max	m	182	m							ν_{26}	CH_3 torsion
139 Q	w									ν_{16}'	C_1SiC_3 bend
132 Q	w	161	m					165	w	ν_{16}	C_1SiC_3 bend
94 R											
87 Q,C	m	150	m							ν_{27}'	CH_2Cl torsion
81 Q										ν_{27}	CH_2Cl torsion
		93	m								lattice modes
		61	m								lattice modes

[a]Abbreviations used: s, strong; m, moderate; w, weak; v, very; bd, broad; sh, shoulder; p, polarized; dp, depolarized. A, B and C refer to infrared band envelopes; P, Q, and R refer to the rotational–vibrational branches, the prime indicates *gauche* modes.

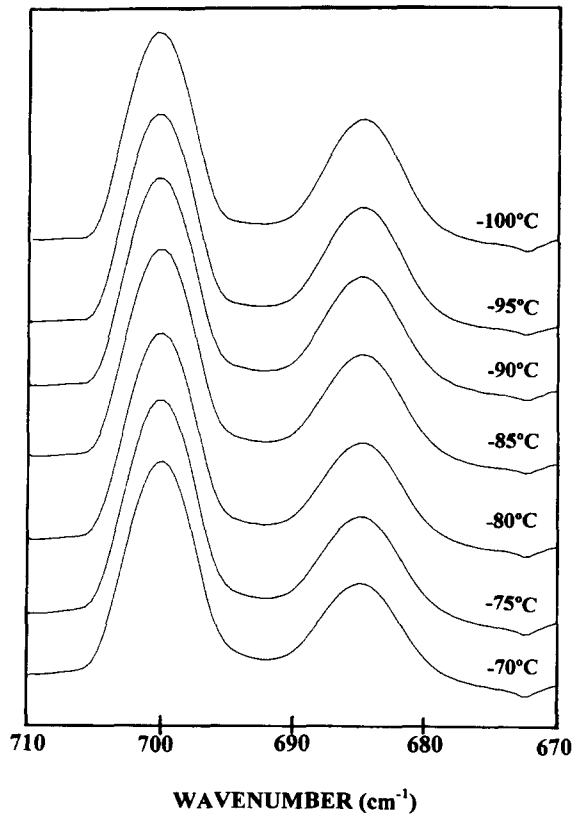

Fig. 7. Temperature dependence of 700 and 685 cm^{-1} infrared bands of chloromethyl methyl silane-d_0 dissolved in liquid xenon.

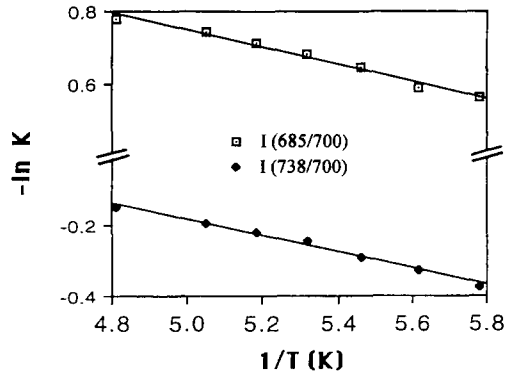

Fig. 8. The van't Hoff plot of the relative intensities of I_{738}/I_{700} and I_{685}/I_{700} cm^{-1} infrared bands in xenon solution.

both conformers have similar sizes but significant differences in polarities.

4. Vibrational assignment

The vibrational assignment of chloromethyl methyl silane was previously reported from an infrared investigation of all phases [7]. However, the present data obtained are at a higher resolution and the band contours are well defined. Additionally, the infrared spectra of the sample dissolved in the xenon matrix solution, the far infrared spectra of the vapor and solid, and the Raman spectra of the liquid and solid phases were recorded for the first time. Because of this, several modes belonging to the *gauche* conformer were observed and clearly assigned and reported in Tables 1 and 2 for the $-d_0$ and $-d_2$ isotopomers, respectively. Group frequencies, infrared gas phase band contours, and Raman depolarization data are utilized along with the normal coordinate analysis from ab initio calculations in the assignment of the spectra. Although the *gauche* conformer is more profound in the fluid phases, it is clear that the *trans* conformer remains in the crystalline state. Therefore, all assignments for the *trans* rotamer are reported from the solid phase data, thus facilitating in the assignment. However, there are some changes in the assignment of the normal modes resulting from the improved data and the normal coordinate analysis that must be noted as well as the assignments obtained from the low frequency data.

The CH_3 antisymmetric stretches (ν_1, ν_{17}) and the CH_2 antisymmetric stretch (ν_{18}) were previously assigned to a single band in the spectra. From our data, there is a weak band observed at 2990 cm^{-1} which is now assigned to the CH_3 antisymmetric stretching modes. Also, the ab initio calculations indicate a reversal in the assignment of the CH_2 rock (ν_{21}) and the CH_2 twist (ν_{23}). Additionally, the ab initio calculations indicate that the band at 620 cm^{-1} previously assigned to the SiH_2 twist of the *gauche* conformer is now assigned to the C–Si stretch of the *gauche* conformer and the band at 579 cm^{-1} is assigned to the SiH_2 twist of both rotamers.

The strong band observed in the spectrum of the gas at 773 cm^{-1} is assigned to the C–Cl stretch. This band is listed in the earlier work, but was unassigned. The

Table 2
Observed infrared[a] and Raman wavenumbers (cm^{-1}) for chloromethyl methyl silane-d_2

Infrared				Raman				Assignment	
Gas	Rel. int.	Solid	Rel. int.	Liquid	Rel. int. and depol.	Solid	Rel. int.	ν_i^b	Approximate description
3101 R									
3085 ctr,B	vw								
3068 P									
2990 R									
2986 Q	m	2990	vw			2993	m	ν_1,ν_{17}	CH_3 antisymmetric stretch
2983 Q	m							ν_{18}'	CH_2 antisymmetric stretch
2978 Q	m	2967	m	2977	bd,w,dp	2972	m	ν_{18}	CH_2 antisymmetric stretch
2974 P									
2948 R									
2945 Q,C	m							ν_2'	CH_2 symmetric stretch
2941 Q	m	2946	m	2939	m,p	2948	m	ν_2	CH_2 symmetric stretch
2936 P									
				2913	m,p			ν_3'	CH_3 symmetric stretch
		2906	w			2910	m	ν_3	CH_3 symmetric stretch
		2155	w						SiHD impurity (*gauche*)
		2141	w						SiHD impurity
1592 Q	vs	1582	vs			1576	w	ν_{19}	SiD_2 antisymmetric stretch
1585 R									
1582 Q								ν_{19}'	SiD_2 antisymmetric stretch
1577 P									
1566 Q	vs	1567	vs	1558	vs,p	1560	vs	ν_4	SiD_2 symmetric stretch
1566 R									
1558 Q	vs							ν_4'	SiD_2 symmetric stretch
1552 P									
1435	bd,sh								
		1428	s	1421	vw,dp	1421	w	ν_{20}	CH_3 antisymmetric deformation
1422 Q	m	1421	s			1414	w	ν_5	CH_3 antisymmetric deformation
1416 R									
1410 Q	m							ν_6'	CH_2 deformation
1401 Q	m	1397	s	1401	bd,w,dp	1393	vw	ν_6	CH_2 deformation
1347									
1343 ctr,B	w	1351	vw						
1338									
1268									
1262 ctr,B	m	1250		1258	w,p	1249	w	ν_7	CH3 symmetric deformation
1257									
1183 R									
1178 Q,A	w	1168	m	1180	vw,p	1177	vw	ν_8	CH_2 wag

1173 P									
		1164	vw						
		1116	vw						
1111 R									
1106 Q,A	w	1107	w	1107	vw,dp	1100	w	ν_{21}	CH_2 rock
1101 P									
828 Q	vs							ν_9'	SiD_2 deformation
823 Q	vs	822	vs	823	bd,vw	827	vw	ν_{22}	CH_3 rock
818 Q	vs	814	vs					ν_9,ν_{22}'	SiD_2 deformation/CH_3 rock
796 Q	s								
786 P		786	w	787	w,p			ν_{23}'	CH_2 twist
				752	w,p	759	vw	ν_{10}	SiD_2 wag
749 R									
743 Q	m	748	vs			749	vs	ν_{23}	CH_2 twist
740 Q	m			738	w,p			ν_{10}'	SiD_2 wag
734 P									
734 R									
729 Q	m	731	s	727	w,p	727	m	ν_{11}	C–Cl stretch
726 Q	m							ν_{12}'	CH_3 rock
722 P									
				703	w,p			ν_{11}'	C–Cl stretch
695 R									
689 Q	s	678	s	686	w,p	678	m	ν_{12}	CH_3 rock
682 P									
645 Q	vw	649	m	641	vs,p	651	m	ν_{13}	C_1–Si stretch
634 Q	m							ν_{13}'	C_1–Si stretch
574 R									
568 Q	w	576	s	572	w,p	574	m	ν_{14}	Si–C_3 stretch
563 P		554	sh						
546 R									
540 Q	m			544	w,p			ν_{14}'	Si–C_3 stretch
536 P									
479 R									
472 Q	w			480	m,p	473	m	ν_{24}	SiD_2 twist
466 P									
408 R									
403 Q	w	393	m	405	w,p	398	vw	ν_{25}	SiD_2 rock
395 P									

Table 2
(*continued*)

Infrared				Raman				Assignment	
Gas	Rel. int.	Solid	Rel. int.	Liquid	Rel. int. and depol.	Solid	Rel. int.	ν_i^b	Approximate description
246 R									
240 Q	s	246	s	243	w,p	250	m	ν_{15}	SiC_3Cl bend
235 P									
157 Q,sh	w			168	bd,w,p			ν_{26}'	CH_3 torsion
147 max	m	180	m					ν_{26}	CH_3 torsion
138 Q	w							ν_{16}'	C_1SiC_3 bend
132 Q	w	156	m			165	w	ν_{16}	C_1SiC_3 bend
90 R									
85 Q,C	m	150	m					ν_{27}'	CH_2Cl torsion
80 Q								ν_{27}	CH_2Cl torsion
79 P									
		90	m			82	m		lattice modes
		61	m			67	s		lattice modes

[a]Abbreviations used: s, strong; m, moderate; w, weak; v, very; bd, broad; sh, shoulder; p, polarized; dp, depolarized. A, B and C refer to infrared band envelopes; P, Q, and R refer to the rotational–vibrational branches; the prime indicates *gauche*-2 modes, and double primes indicate *cis* modes.

Table 3
Temperature and intensity ratios for the conformational study of chloromethyl methyl silane in liquid xenon

T (°C)	T (K)	1000/T (K)	I_{685}/I_{700}	−ln$K$	I_{738}/I_{700}	−ln$K$
−70	203	4.926	0.4587	0.7795	1.159	−0.1479
−75	198	5.051	0.4759	0.7426	1.211	−0.1916
−80	193	5.181	0.4895	0.7144	1.242	−0.2168
−85	188	5.319	0.5058	0.6816	1.281	−0.2473
−90	183	5.464	0.5260	0.6424	1.339	−0.2921
−95	178	5.618	0.5561	0.5868	1.388	−0.3278
−100	173	5.780	0.5701	0.5619	1.454	−0.3747
				181 ± 6		180 ± 5

[a]Average ΔH = 180 ± 4 (516 ± 11 cal mol^{-1}).

bands previously assigned to the C–Si stretches at 740 and 728 cm^{-1} were not observed in our spectra and thus must have been due to impurities in the earlier sample [7]. However, the bands at 701 and 685 cm^{-1} formerly assigned [7] to the C–Cl stretching modes of the *trans* and *gauche* conformers, respectively, are now assigned to the C–Si stretching modes, respectively.

Additional vibrational data is provided by the far infrared spectra of the vapor and solid phases and from the low frequency Raman spectra of the liquid and solid. The SiCCl bend for the *trans* conformer is assigned to the band observed at 246 cm^{-1} in the gas and liquid phases, and at 249 and 253 cm^{-1} for the solid phases of the infrared and Raman spectra, respectively. The shoulder observed at 255 cm^{-1} in the Raman spectrum of the liquid is assigned to the corresponding *gauche* vibration. The methyl torsion of the *trans* conformer, ν_{26}, was observed as a band of medium intensity in the infrared spectra of the gas and solid at 154 and 161 cm^{-1}, respectively, and as a very weak line at 165 cm^{-1} in the Raman spectrum of the solid. The corresponding mode for the *gauche* form is assigned to a very weak line at 178 cm^{-1} (Raman spectrum of the liquid) and a shoulder at 175 cm^{-1} (infrared spectrum of the vapor). The two remaining fundamentals are the CSiC bend and the asymmetric torsional mode. The CSiC bend is assigned to the band at 150 cm^{-1} (infrared solid) for the *trans* conformer, and at 139 cm^{-1} (infrared vapor) for the *gauche* form. The asymmetric torsional mode was observed in the infrared spectrum of the gas at 87 cm^{-1} for the *gauche* conformer and a higher frequency of 112 cm^{-1} in the spectrum of the solid is assigned to the corresponding mode for the *trans* rotamer.

In the deuterated analogue, there are some differences in our proposed assignments compared to the earlier one [7] that should be noted. The CH_3 antisymmetric stretches, ν_1 and ν_{17}, are interchanged with the assignment of the CH_2 antisymmetric stretch, ν_{18}. The ab initio calculations still indicate a reversal of the CH_2 rock and CH_2 twist vibrations, but also indicate a reversal of the assignment of the SiD_2 wag and the SiC stretch. Additionally, the SiD_2 deformation previously assigned at 728 cm^{-1} is now assigned to the band at 818 cm^{-1} along with the CH_3 rock of the *gauche* conformer (ν_{22}'). The band at 728 cm^{-1} is now assigned to the C–Cl stretch, and the band at 689 cm^{-1} (previously the CCl stretch) is now assigned as the CH_3 rock (ν_{12}), according to the ab initio calculations. The remaining four fundamentals below 400 cm^{-1} are assigned similar to those in the normal compound.

5. Ab initio calculations

The LCAO-MO-SCF restricted Hartree–Fock calculations were performed with the Gaussian-92 program [11] using Gaussian-type basis functions. The energy minima with respect to nuclear coordinates were obtained by the simultaneous relaxation of all of the geometric parameters using the gradient method of Pulay [12]. The structural optimization for both the *trans* and the *gauche* conformers were carried out with initial parameters taken from those of 1,1-dichloropropane [13] and dichlorodimethylsilane [14]. The 3-21G* and 6-31G* basis sets were employed at the level of restricted Hartree–Fock (RHF) and Moller–Plesset (MP2) to second order. The determined structural parameters are listed in Table 4.

Table 4
Structural parameters, rotational constants, dipole moments, and energy for chloromethyl methyl silane

	RHF/3-21G*		RHF/6-31G*		MP2/6-31G*		MP2/6-311 + G**	
Parameter	*gauche*	*trans*	*gauche*	*trans*	*gauche*	*trans*	*gauche*	*trans*
Si_2-C_1	1.876	1.882	1.882	1.888	1.874	1.880	1.868	1.874
C_3-Si	1.897	1.897	1.905	1.904	1.897	1.896	1.891	1.891
$Cl-C_3$	1.830	1.828	1.804	1.801	1.794	1.792	1.791	1.790
H_5-C_1	1.087	1.087	1.086	1.086	1.093	1.093	1.093	1.094
H_6-C_1	1.086	1.087	1.085	1.087	1.094	1.093	1.092	1.093
H_7-C_1	1.087	1.087	1.086	1.087	1.093	1.093	1.094	1.093
H_8-Si	1.480	1.474	1.480	1.475	1.490	1.485	1.481	1.476
H_9-Si	1.474	1.474	1.475	1.475	1.485	1.485	1.477	1.476
$H_{10}-C_3$	1.081	1.081	1.081	1.081	1.092	1.092	1.091	1.092
$H_{11}-C_3$	1.081	1.081	1.081	1.081	1.092	1.092	1.092	1.092
C_3SiC_1	111.3	109.4	111.4	109.3	110.6	109.1	110.2	109.2
ClC_3Si	110.2	109.9	111.6	111.3	111.1	111.3	111.1	111.6
H_5C_1Si	110.8	110.8	110.7	110.7	111.0	110.8	111.1	110.9
H_6C_1Si	110.9	111.4	111.2	111.5	110.6	111.2	110.8	111.2
H_7C_1Si	111.3	111.4	111.3	111.5	111.0	111.2	110.8	111.2
H_8SiC_3	106.5	108.3	106.3	108.5	106.7	108.4	106.9	108.3
H_9SiC_3	108.1	108.3	108.4	108.5	108.3	108.4	108.5	108.3
$H_{10}C_3Si$	112.4	112.7	111.8	112.0	111.6	111.5	111.6	111.3
$H_{11}C_3Si$	112.8	112.7	112.1	112.0	111.5	111.5	111.1	111.3
ClC_3SiC_1	61.4	180.0	61.5	180.0	59.7	180.0	58.7	180.0
$H_5C_1SiC_3$	−179.4	180.0	−179.8	180.0	−179.8	180.0	−179.3	180.0
$H_6C_1SiH_3$	119.9	119.7	119.9	119.7	120.0	119.8	120.2	119.8
$H_7C_1SiH_5$	−120.2	−119.7	−120.4	−119.7	−120.0	−119.8	−119.9	−119.8
$H_8SiC_3C_1$	120.8	120.9	120.5	120.7	120.8	120.8	118.1	120.7
$H_9SiC_3C_1$	−122.4	−120.9	−122.8	−120.7	−122.2	−120.8	−120.3	−120.7
$H_{10}C_3SiCl$	118.2	118.4	119.2	119.3	119.8	119.8	120.0	120.0
$H_{11}C_3SiCl$	−118.6	−118.4	−119.4	−119.3	−119.6	−119.8	−119.7	−120.0
A	7750	15560	7763	15550	7681	15702	7784	15804
B	2292	17077	2237	1705	2289	1741	2353	1748
C	1950	1598	1910	1595	1941	1629	1988	1636
$\|\mu_a\|$	1.724	2.644	1.683	2.552	1.597	2.517	1.573	2.464
$\|\mu_b\|$	0.831	−1.378	0.793	1.319	0.770	1.333	0.813	1.287
$\|\mu_c\|$	0.961	0.000	0.924	0.000	0.917	0.000	0.881	0.000
$\|\mu_t\|$	2.142	2.982	2.077	2.873	2.000	2.849	1.978	2.780
$-(E + 824)$	0.279905	0.279114	4.216001	4.215428	4.716628	4.717433	5.052083	5.051076
ΔE (cm^{-1})		174		126		176		221

In order to obtain a more complete description of the molecular motions involved in the normal modes of $ClCH_2SiH_2CH_3$, we have carried out a normal coordinate analysis. The force fields in Cartesian coordinates were calculated by the Gaussian-92 program [11] with the MP2/6-31G* basis set. Internal coordinates (Fig. 9) were used to calculated the G and B matrices using the structural parameters given in Table 4. Using the B matrix, [15] the force field in Cartesian coordinates was then converted to a force field in internal coordinates, and the pure ab initio vibrational frequencies were reproduced. The force constants for the *trans* and *gauche* conformers can be obtained from the authors. Subsequently, scaling factors of 0.9 for stretching and bending and 1.0 for the torsional coordinates, and the geometric average of scaling factors for interaction force constants were used to obtain the fixed scaled force field and resultant wavenumbers. A set of symmetry coordinates was used (Table 5) to determine the corresponding potential energy distributions (PED). A comparison between the observed and calculated frequencies of

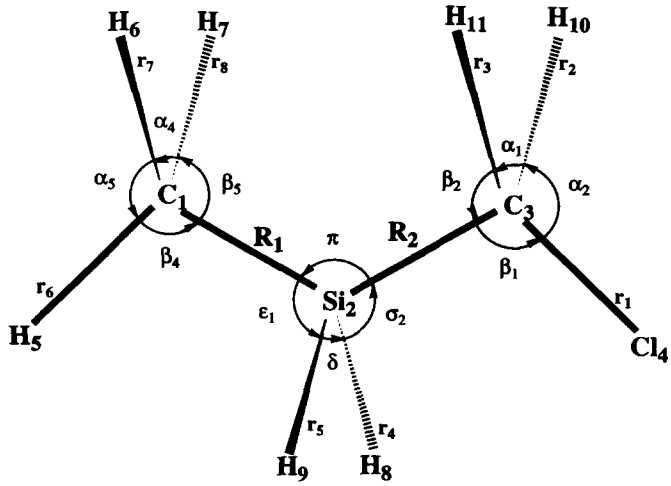

Fig. 9. Internal coordinates of chloromethyl methyl silane.

Table 5
Symmetric coordinates for chloromethyl methyl silane

Species	Description	Symmetry coordinate
A′	CH_3 antisymmetric stretch	$S_1 = 2r_6 - r_7 - r_8$
	CH_2 symmetric stretch	$S_2 = r_2 + r_3$
	CH_3 symmetric stretch	$S_3 = r_6 + r_7 + r_8$
	SiH_2 symmetric stretch	$S_4 = r_4 + r_5$
	CH_3 antisymmetric deformation	$S_5 = 2\alpha_4 - \alpha_5 - \alpha_6$
	CH_2 deformation	$S_6 = 4\alpha_1 - \alpha_2 - \alpha_3 - \beta_2 - \beta_3$
	CH_3 symmetric deformation	$S_7 = \alpha_4 + \alpha_5 + \alpha_6 - \beta_4 - \beta_5 - \beta_6$
	CH_2 wag	$S_8 = \beta_2 + \beta_3 - \alpha_2 - \alpha_3$
	SiH_2 deformation	$S_9 = 4\delta - \epsilon_1 - \epsilon_2 - \sigma_1 - \sigma_2$
	SiH_2 wag	$S_{10} = \epsilon_1 + \epsilon_2 - \sigma_1 - \sigma_2$
	C–Cl stretch	$S_{11} = r_1$
	CH_3 rock	$S_{12} = 2\beta_4 - \beta_5 - \beta_6$
	C_1–Si stretch	$S_{13} = R_1$
	SiC_3 stretch	$S_{14} = R_2$
	SiC_3Cl bend	$S_{15} = 5\beta_1 - \alpha_1 - \alpha_2 - \alpha_3 - \beta_2 - \beta_3$
	C_1SiC_3 bend	$S_{16} = 5\pi - \delta - \epsilon_1 - \epsilon_2 - \sigma_1 - \sigma_2$
A″	CH_3 antisymmetric stretch	$S_{17} = r_7 - r_8$
	CH_2 antisymmetric stretch	$S_{18} = r_2 - r_3$
	SiH_2 antisymmetric stretch	$S_{19} = r_4 - r_5$
	CH_3 antisymmetric deformation	$S_{20} = \alpha_5 - \alpha_6$
	CH_2 rock	$S_{21} = \alpha_2 - \alpha_3 + \beta_2 - \beta_3$
	CH_3 rock	$S_{22} = \beta_5 - \beta_6$
	CH_2 twist	$S_{23} = \alpha_2 - \alpha_3 - \beta_2 + \beta_3$
	SiH_2 twist	$S_{24} = \epsilon_1 - \epsilon_2 - \sigma_1 + \sigma_2$
	SiH_2 rock	$S_{25} = \epsilon_1 - \epsilon_2 - \sigma_1 - \sigma_2$
	CH_3 torsion	$S_{26} = \tau_1$
	CH_2Cl torsion	$S_{27} = \tau_2$

Table 6
Observed and calculated frequencies for *trans* and *gauche* chloromethyl methyl silane-d_0

Species	Fundamental	*Ab initio*[a]	Fixed scaled[b]	IR int.[c]	Raman act.[d]	dp ratio	Obs.[e]	PED
trans								
$A'\nu_1$	CH_3 antisymmetric stretch	3205	3041	4.9	114.9	0.75	2992	$100S_1$
ν_2	CH_2 symmetric stretch	3141	2980	9.7	79.0	0.06	2946	$100S_2$
ν_3	CH_3 symmetric stretch	3110	2950	1.7	113.8	0.01	2910	$100S_3$
ν_4	SiH_2 symmetric stretch	2313	2194	96.7	139.2	0.07	2144	$100S_4$
ν_5	CH_3 antisymmetric deformation	1525	1447	4.2	17.4	0.74	1416	$94S_5$
ν_6	CH_2 deformation	1507	1430	8.0	9.0	0.75	1406	$99S_6$
ν_7	CH_3 symmetric deformation	1375	1305	26.1	0.7	0.18	1248	$98S_7$
ν_8	CH_2 wag	1282	1216	6.7	0.8	0.39	1180	$97S_8$
ν_9	SiH_2 deformation	994	943	101.8	15.5	0.75	954	$98S_4$
ν_{10}	SiH_2 wag	946	898	223.1	4.1	0.69	905	$57S_{10},35S_{12}$
ν_{11}	C–Cl stretch	811	769	2.0	6.6	0.16	762	$66S_{11},22S_{14}$
ν_{12}	CH_3 rock	796	755	47.2	22.7	0.64	749	$31S_{12},33S_{10},18S_{14}$
ν_{13}	C_1–Si stretch	724	686	21.7	3.9	0.34	700	$79S_{13},10S_{11}$
ν_{14}	SiC_3 stretch	638	605	17.7	20.6	0.17	608	$39S_{14},19S_{11},19S_{12}$
ν_{15}	SiCCl bend	248	235	1.6	4.4	0.43	249	$47S_{15}, 32S_{16}$
ν_{16}	CSiC bend	140	133	2.0	0.1	0.75	132*	$56S_{16},41S_{15}$
$A''\nu_{17}$	CH_3 antisymmetric stretch	3205	3041	3.6	74.8	0.75	2992	$91S_{17}$
ν_{18}	CH_2 antisymmetric stretch	3208	3043	5.2	70.3	0.75	2973	$90S_{18},10S_{17}$
ν_{19}	SiH_2 antisymmetric stretch	2321	2202	166.6	56.9	0.75	2167	$100S_{19}$
ν_{20}	CH_3 antisymmetric deformation	1526	1447	6.1	16.8	0.75	1427	$96S_{20}$
ν_{21}	CH_2 rock	1188	1127	0.9	11.0	0.75	1099	$92S_{21}$
ν_{22}	CH_3 rock	929	882	45.6	8.3	0.75	874	$63S_{22},21S_{24}$
ν_{23}	CH_2 twist	869	825	31.8	5.9	0.75	810	$55S_{23},29S_{24},14S_{25}$
ν_{24}	SiH_2 twist	595	565	0.3	4.1	0.75	584*	$50S_{24},24S_{23},22S_{22}$
ν_{25}	SiH_2 rock	476	454	10.8	0.2	0.75	470	$66S_{25},12S_{23},10S_{22}$
ν_{26}	CH_3 torsion	161	161	0.0	0.0	0.75	154*	$96S_{25}$
ν_{27}	CH_2Cl torsion	81	81	1.2	0.5	0.75	80*	$94S_{21}$
gauche								
$A'\nu_1$	CH_3 antisymmetric stretch	3206	3042	3.6	105.4	0.63	2986	$71S_1,30S_{18}$
ν_2	CH_2 symmetric stretch	3144	2982	2.7	79.4	0.10	2966	$100S_2$
ν_3	CH_3 symmetric stretch	3113	2953	12.8	108.9	0.02	2917	$100S_3$
ν_4	SiH_2 symmetric stretch	2289	2172	67.9	121.1	0.26	2144	$63S_4,37S_{19}$
ν_5	CH_3 antisymmetric deformation	1526	1447	5.0	11.0	0.74	1417	$73S_5,23S_{20}$
ν_6	CH_2 deformation	1506	1428	5.7	19.2	0.75	1412	$94S_6$
ν_7	CH_3 symmetric deformation	1375	1304	19.1	0.7	0.13	1256	$98S_7$
ν_8	CH_2 wag	1281	1215	10.1	0.9	0.23	1176	$97S_8$
ν_9	SiH_2 deformation	991	940	159.4	18.3	0.75	942	$97S_9$
ν_{10}	SiH_2 wag	955	906	226.3	6.7	0.73	888	$61S_{10},28S_{12}$
ν_{11}	C–Cl stretch	812	771	0.5	15.4	0.54	764	$64S_{11},28S_{14}$
ν_{12}	CH_3 rock	779	739	25.1	6.3	0.64	738	$11S_{12},25S_{24},16S_{13},14S_{14},12S_{25}$
ν_{13}	C_1–Si stretch	705	668	2.5	14.5	0.52	685	$68S_{13}$
ν_{14}	SiC_3 stretch	644	611	42.1	5.2	0.22	618	$13S_{14},33S_{23},17S_{10},13S_{12}$
ν_{15}	SiCCl bend	256	243	7.2	1.3	0.67	246	$42S_{15},41S_{16}$
ν_{16}	CSiC bend	146	142	4.8	0.2	0.65	139	$22S_{16},40S_{26},31S_{15}$

A'' ν_{17}	CH_3 antisymmetric stretch	3210	3045	9.3	66.7	0.75	2984	$100S_{17}$
ν_{18}	CH_2 antisymmetric stretch	3215	3050	5.4	77.3	0.74	2977	$70S_{18},30S_{17}$
ν_{19}	SiH_2 antisymmetric stretch	2316	2197	88.1	109.7	0.16	2167	$63S_{19},37S_4$
ν_{20}	CH_3 antisymmetric deformation	1523	1445	7.4	10.8	0.74	1430	$68S_{20},22S_5$
ν_{21}	CH_2 rock	1188	1127	13.9	8.4	0.75	1104	$91S_{21}$
ν_{22}	CH_3 rock	935	887	5.8	8.4	0.75	865	$62S_{22},24S_{24},11S_{25}$
ν_{23}	CH_2 twist	869	824	11.7	15.4	0.54	810	$43S_{23},27S_{12}$
ν_{24}	SiH_2 twist	601	571	4.8	3.5	0.64	580	$33S_{24},28S_{14},19S_{11},12S_{22}$
ν_{25}	SiH_2 rock	497	473	89.1	2.9	0.30	486	$63S_{25},15S_{22}$
ν_{26}	CH_3 torsion	175	171	8.3	0.5	0.53	160*	$51S_{26},21S_{15},21S_{16},12S_{27}$
ν_{27}	CH_2Cl torsion	87	86	6.1	1.0	0.75	87	$83S_{27}$

[a]Calculated with the MP2/6-31G* basis set.

[b]Scaling factors of 0.9 for stretching and bending coordinates and 1.0 for torsional coordinates.

[c]Calculated infrared intensities in km mol^{-1} at the MP2/6-31G* level.

[d]Calculated Raman activities in $Å^4$ amu^{-1}, using RHF/6-31G* level.

[e]Frequencies of the *trans* conformer are obtained from the solid except those marked with an asterisk are taken from the spectra of the xenon solution or gas. Frequencies of the *gauche* conformer are taken from the gas or xenon solution.

Table 7
Observed and calculated frequencies for *trans* and *gauche* chloromethyl methyl silane-d_2

Species		Fundamental	Ab initio[a]	Fixed scaled[b]	IR int.[c]	Raman act.[d]	dp ratio	Obs.[e]	PED
trans									
A′	ν_1	CH_3 antisymmetric stretch	3205	3041	4.8	115.2	0.75	2990	$100S_1$
	ν_2	CH_2 symmetric stretch	3141	2980	9.6	79.0	0.06	2946	$100S_2$
	ν_3	CH_3 symmetric stretch	3110	2950	1.7	113.2	0.01	2906	$100S_3$
	ν_4	SiD_2 symmetric stretch	1655	1570	61.5	67.7	0.07	1567	$100S_4$
	ν_5	CH_3 antisymmetric deformation	1525	1447	5.2	17.8	0.75	1421	$95S_5$
	ν_6	CH_2 deformation	1507	1430	7.6	9.0	0.75	1397	$99S_6$
	ν_7	CH_3 symmetric deformation	1375	1304	23.1	1.0	0.12	1250	$98S_7$
	ν_8	CH_2 wag	1280	1214	4.2	1.0	0.34	1168	$98S_8$
	ν_9	SiD_2 deformation	884	839	107.9	1.6	0.71	814	$64S_9,13S_{13},11S_{14}$
	ν_{10}	SiD_2 wag	812	770	2.7	20.4	0.52	759	$65S_{10},10S_9,20S_{13}$
	ν_{11}	C–Cl stretch	755	716	92.3	8.3	0.19	731	$57S_{11},28S_{12}$
	ν_{12}	CH_3 rock	701	665	26.7	5.5	0.57	678	$53S_{12},12S_{10},25S_{11}$
	ν_{13}	C_1–Si stretch	671	636	6.1	8.3	0.25	649	$43S_{13},16S_{12},19S_{14}$
	ν_{14}	SiC_3 stretch	584	554	52.2	17.2	0.30	576	$59S_{14},13S_9,13S_{11}$
	ν_{15}	SiC_3Cl bend	244	231	1.2	4.2	0.44	246	$44S_{15},34S_{16}$
	ν_{16}	C_1SiC_3 bend	137	130	1.8	0.1	0.75	132*	$54S_{16},43S_{15}$
A″	ν_{17}	CH_3 antisymmetric stretch	3205	3041	3.5	75.5	0.75	2990	$91S_{17}$
	ν_{18}	CH_2 antisymmetric stretch	3207	3043	4.8	70.8	0.75	2967	$91S_{18}$
	ν_{19}	SiD_2 antisymmetric stretch	1678	1592	99.0	28.3	0.75	1582	$100S_{19}$
	ν_{20}	CH_3 antisymmetric deformation	1526	1447	7.3	16.7	0.75	1428	$96S_{20}$
	ν_{21}	CH_2 rock	1185	1124	0.2	10.0	0.75	1107	$92S_{21}$
	ν_{22}	CH_3 rock	886	843	48.8	3.8	0.75	822	$72S_{22},13S_{25}$
	ν_{23}	CH_2 twist	804	763	9.0	3.6	0.75	748	$66S_{23},16S_{24}$
	ν_{24}	SiD_2 twist	468	444	0.1	4.2	0.75	473	$80S_{24}$
	ν_{25}	SiD_2 rock	385	366	7.6	0.3	0.75	393	$77S_{25}$
	ν_{26}	CH_3 torsion	161	161	0.0	0.0	0.75	147*	$97S_{26}$
	ν_{27}	CH_2Cl torsion	80	79	1.3	0.5	0.75	79*	$95S_{27}$

gauche									
A′	ν_1	CH_3 antisymmetric stretch	3206	3042	3.7	105.8	0.63	2986	$71S_1,30S_{18}$
	ν_2	CH_2 symmetric stretch	3144	2982	2.6	79.1	0.10	2945	$100S_2$
	ν_3	CH_3 symmetric stretch	3113	2953	12.7	108.3	0.02	2913*	$100S_3$
	ν_4	SiD_2 symmetric stretch	1642	1558	33.3	73.0	0.14	1558	$87S_4,12S_{19}$
	ν_5	CH_3 antisymmetric deformation	1526	1447	5.0	11.1	0.75	1422	$72S_5,24S_{20}$
	ν_6	CH_2 deformation	1505	1428	5.3	19.3	0.75	1410	$95S_6$
	ν_7	CH_3 symmetric deformation	1374	1303	16.6	1.0	0.08	1262	$98S_7$
	ν_8	CH_2 wag	1280	1214	8.4	1.1	0.19	1178	$98S_8$
	ν_9	SiD_2 deformation	893	847	61.0	2.6	0.74	828*	$38S_9,23S_{22}$
	ν_{10}	SiD_2 wag	793	753	12.5	13.1	0.65	738*	$51S_{10},11S_{13},11S_{14}$
	ν_{11}	C–Cl stretch	738	670	28.4	7.5	0.62	703	$37S_{11},10S_{10},19S_{23}$
	ν_{12}	CH_3 rock	718	682	70.4	10.0	0.60	689	$77S_{12}$
	ν_{13}	C_1–Si stretch	658	624	2.4	17.4	0.13	634	$24S_{13},40S_{11},15S_{12}$
	ν_{14}	SiC_3 stretch	550	522	55.9	6.1	0.54	540	$66S_{14},10S_{23}$
	ν_{15}	SiC_3Cl bend	144	140	3.7	0.3	0.63	240	$38S_{15},25S_{16},29S_{26}$
	ν_{16}	C_1SiC_3 bend	246	234	7.1	1.2	0.70	138	$45S_{16},34S_{15}$
	ν_{17}	CH_3 antisymmetric stretch	3215	3050	5.6	77.5	0.74	2986	$70S_{17},30S_{18}$
	ν_{18}	CH_2 antisymmetric stretch	3210	3045	9.3	67.2	0.75	2983	$100S_{18}$
	ν_{19}	SiD_2 antisymmetric stretch	1670	1585	66.4	39.9	0.38	1582	$88S_{19},12S_4$
	ν_{20}	CH_3 antisymmetric deformation	1523	1445	8.0	11.0	0.75	1421	$67S_{20},23S_5$
	ν_{21}	CH_2 rock	1186	1125	11.3	8.9	0.75	1106	$91S_{21}$
	ν_{22}	CH_3 rock	884	838	44.2	2.5	0.75	823	$48S_{22},27S_9$
	ν_{23}	CH_2 twist	836	793	37.6	3.4	0.29	796	$31S_{23},15S_{10},18S_{11},17S_{13},11S_{14}$
	ν_{24}	SiD_2 twist	486	461	0.4	9.0	0.45	472	$72S_{24}$
	ν_{25}	SiD_2 rock	409	388	59.3	1.6	0.43	403	$68S_{25},11S_{22}$
	ν_{26}	CH_3 torsion	170	167	11.1	0.3	0.53	157	$64S_{26},11S_{15},14S_{16}$
	ν_{27}	CH_2Cl torsion	84	84	5.7	1.0	0.75	87	$87S_{27}$

[a]Calculated with the MP2/6-31G* basis set.

[b]Scaling factors of 0.9 for stretching and bending coordinates and 1.0 for torsional coordinates.

[c]Calculated infrared intensities in km mol^{-1} at the MP2/6-31G* level.

[d]Calculated Raman activities in $Å^4$ amu^{-1}, using RHF/6-31G* level.

[e]Frequencies of the *trans* conformer are obtained from the solid except those marked with an asterisk are taken from the spectra of the xenon solution or gas. Frequencies of the *gauche* conformer are taken from the gas or xenon solution.

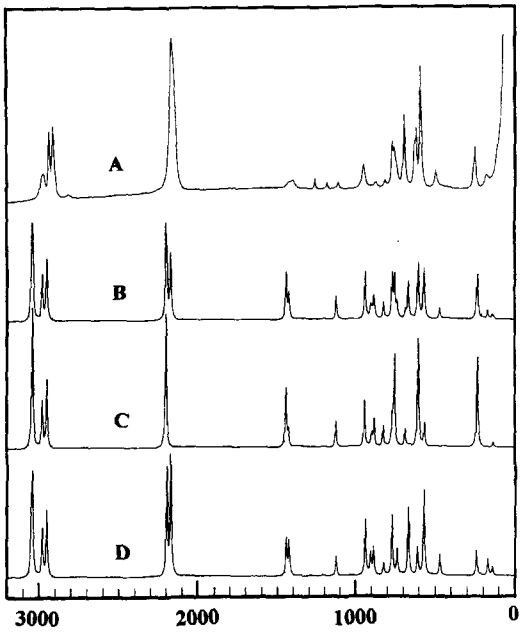

Fig. 10. Predicted and observed Raman spectra of chloromethyl methyl silane-d_0: (A) observed spectrum of liquid; (B) predicted spectrum of mixture of *gauche* and *trans* conformers with ΔH = 180 cm^{-1}; (C) predicted spectrum of pure *trans* conformer; and (D) predicted spectrum of pure *gauche* conformer.

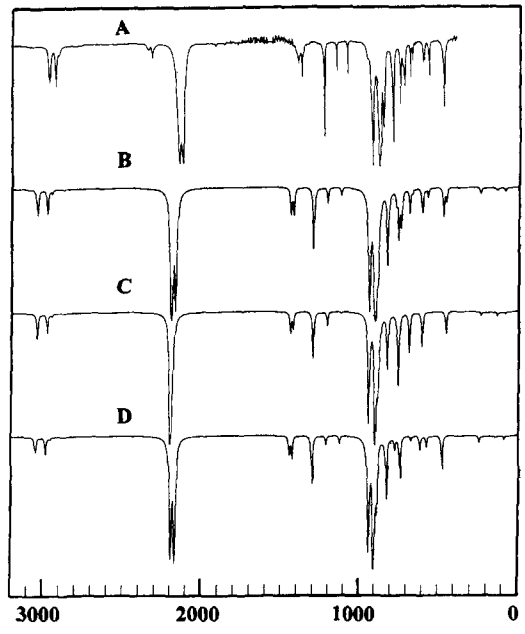

Fig. 11. Predicted and observed infrared spectra of chloromethyl methyl silane-d_0: (A) observed spectrum of xenon solution; (B) predicted spectrum of mixture of *gauche* and *trans* conformers with ΔH = 180 cm^{-1}; (C) predicted spectrum of pure *trans* conformer; and (D) predicted spectrum of pure *gauche* conformer.

chloromethyl methyl silane along with the calculated infrared intensities, Raman activities, depolarization ratios and PED are given in Table 6 and Table 7 for d_0 and d_2, respectively.

The predicted Raman and infrared spectra (Figs. 10–13) for chloromethyl methyl silane were calculated using the frequencies, scattering activities and intensities determined from the ab initio calculations. The Gaussian-92 program [11] with the option of calculating the polarizability derivatives was used. The Raman scattering cross sections, $\partial\sigma_j/\partial\Omega$, which are proportional to the Raman intensities, can be calculated from the scattering activities and the predicted frequencies for each normal mode using the relationship: [16]

$$\frac{\partial\sigma_j}{\partial\Omega}=\left(\frac{2^4\pi^4}{45}\right)\left(\frac{(\nu_0-\nu_j)^4}{1-\exp\left[\frac{-hc\nu_j}{kT}\right]}\right)\left(\frac{h}{8\pi^2 c\nu_j}\right)S_j$$

where ν_0 is the exciting frequency, ν_j is the vibrational frequency of the jth normal mode, h, c and k are universal constants, and S_j is the corresponding Raman scattering activity. To obtain the polarized Raman scattering cross section, the polarizabilities are incorporated into S_j by $S_j[(1-\rho_j)/(1+\rho_j)]$ where ρ_j is the depolarization ratio of the jth normal mode. The Raman scattering cross sections and calculated frequencies are used together with a Lorentzian line shape function to obtain the calculated spectrum. Since the calculated frequencies are $\approx$ 10% higher than those observed, the frequency axis of the theoretical spectrum was compressed by a factor of 0.9. The predicted Raman spectra of the *trans* and *gauche* pure conformers are shown in Fig. 10(C) and (D) respectively for the normal species, and Fig. 12(C) and (D) for the Si-d_2 isotopomer. The corresponding predicted Raman spectra of the mixture of the two conformers with an assumed ΔH of 180 cm^{-1} are shown in Fig. 10(B) and Fig. 12(B), respectively. These spectra should be compared to the experimental spectra of the liquids (Fig. 10(A) and Fig. 12(A)). The calculated

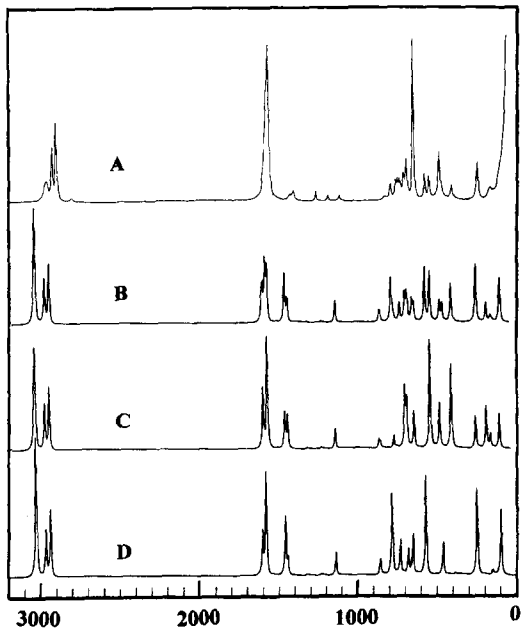

Fig. 12. Predicted and observed Raman spectra of chloromethyl methyl silane-d_2: (A) observed spectrum of liquid; (B) predicted spectrum of mixture of *gauche* and *trans* conformers with ΔH = 180 cm^{-1}; (C) predicted spectrum of pure *trans* conformer; and (D) predicted spectrum of pure *gauche* conformer.

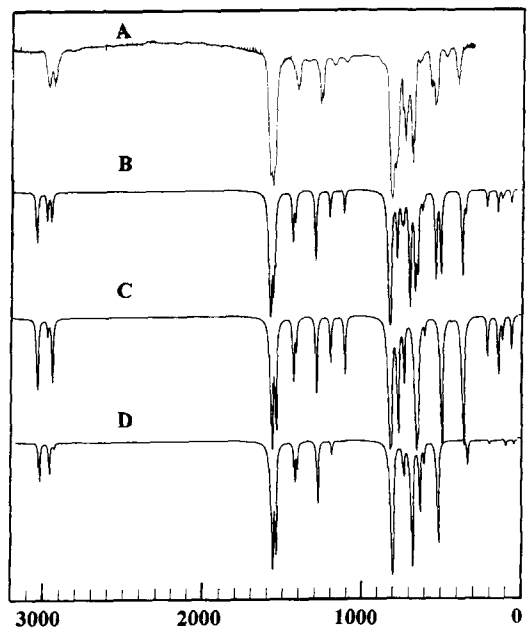

Fig. 13. Predicted and observed infrared spectra of chloromethyl methyl silane-d_2: (A) observed spectrum of gas; (B) predicted spectrum of mixture of *gauche* and *trans* conformers with ΔH = 180 cm^{-1}; (C) predicted spectrum of pure *trans* conformer; and (D) predicted spectrum of pure *gauche* conformer.

Raman spectra are quite similar to the experimental spectra with the exception of the intensities of the higher wavenumber carbon–hydrogen stretches of the CH_3 deformation, which are predicted too strong, and the Si–C stretches which are predicted too weak. Similar problems are encountered in the calculated spectra of the Si-d_2 isotopomer. Nevertheless, the calculated spectra are considered to be in reasonable agreement with the observed spectra and demonstrates the value of using the calculated intensities to aid in the vibrational assignment even at the relatively low level of the calculation.

Infrared intensities were also calculated based on the dipole moment derivatives with respect to the Cartesian coordinates. The derivatives were taken from the ab initio calculations at the MP2/6-31G* level and transformed to normal coordinates by:

$$\left(\frac{\partial \mu_\mu}{\partial Q_i}\right) = \sum_j \left(\frac{\partial \mu_\mu}{\partial X_i}\right) L_{ji}$$

where the Q_i is the ith normal coordinate, X_j is the jth Cartesian displacement coordinates, L_{ji} is the transformation matrix between the Cartesian displacement coordinates and normal coordinates. The infrared intensities were then calculated by

$$I_i = \frac{N\pi}{3c^2}\left[\left(\frac{\partial \mu_x}{\partial Q_i}\right)^2 + \left(\frac{\partial \mu_y}{\partial Q_i}\right)^2 + \left(\frac{\partial \mu_z}{\partial Q_i}\right)^2\right]$$

In Fig. 11(C) and (D), the predicted infrared spectra of the two conformers of the normal species are shown, whereas in Fig. 13(C) and (D) the predicted infrared spectra of the Si-d_2 isotopomer are shown. The combination of the spectra of the two conformers with a ΔH of 180 cm^{-1} are shown in Figs. 12(B) and 13(B). The experimental infrared spectrum of the normal species dissolved in liquid xenon at −70° is also shown for comparison in Fig. 11(A) and the infrared spectrum of gaseous Si-d_2 sample is shown in Fig. 13(A). Excluding the overtones or combination bands which are present in the spectrum of the xenon solution, the agreement between the observed and

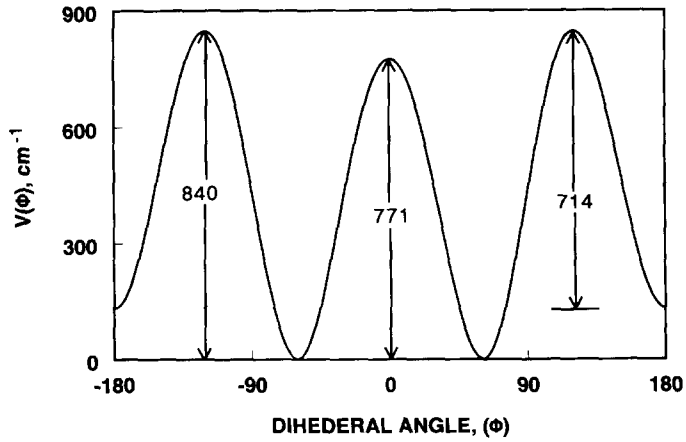

Fig. 14. Potential function governing internal rotation of chloromethyl methyl silane as determined by ab initio calculations with RHF/6-31G* basis set. The potential surface calculated by allowing for optimization at transition states as well as the *gauche* position by relaxation of all geometric parameters.

calculated spectra for both the d_0 and Si-d_2 isotopomers are considered satisfactory and provide support for the vibrational assignments.

The potential surface (Fig. 14) of the asymmetric torsion was obtained by relaxation of all structural parameters in the expected potential minima and maxima using the MP2/6-31G* basis set. The calculated energy difference of 176 cm^{-1} from the MP2/6-31G* calculation with the *gauche* conformer more stable is in agreement with the experimental results from the variable temperature study. The relative energies of the potential barriers appear to have reasonable values based on the barriers to internal rotation of some similar molecules.

6. Discussion

In the previous study [7] of chloromethyl methyl silane, the large overlap of bands in the gaseous state and the observation of no appreciable changes in the spectra of the liquid between 23 and −100°C made it impossible for the investigators to determine the thermodynamically preferred conformer in the fluid states. In the present study, an alternative method to determine the ΔH value was performed by using a very low concentration of the sample dissolved in an inert liquid matrix of xenon atoms. Since liquified noble gases are the most inert solvents, only small interactions are expected to occur between the sample and the surrounding atoms, and the enthalpy differences of conformers which have similar size and polarity of samples dissolved in such solutions are expected to be comparable to those in the gas phase [9,10]. The measurement of the infrared spectrum of the liquified noble gas solution as a function of temperature provides a convenient way to determine the ΔH values of compounds that are difficult to obtain in the gas phase. Additionally, the separation of the bands is better than in the infrared spectrum of the gas due to the collapse of the P and R branches. This results in the narrowing of spectral bands and the low temperature reduces excited state transitions ('hot bands') which can easily be mistaken as conformer bands in the infrared spectrum of the gas. These advantages greatly facilitated the analyses and interpretation of the spectra of the molecules of the rare gas solutions. Therefore, we were able to identify more confidently the assignment of the conformer pairs.

Utilizing the predictions from the ab initio calculations it was necessary to revise the previously reported [7] vibrational assignment. Fundamentals below 400 cm^{-1} had not been previously reported so the spectroscopic data in the low wavenumber region is new information. Using a single scaling factor of 0.9 except for the two torsions, the wavenumbers for the fundamentals are predicted from the MP2/6-31G* calculation to 1.8% for the *gauche* conformer and 1.7% for the *trans* conformer. Therefore, ab initio

calculations at this level provide excellent predictions of the wavenumbers for the fundamentals for these types of molecules.

In support of the vibrational assignment the Teller–Redlich product rule was calculated. For the *gauche* conformer the theoretical tau value is 7.24 and the experimental value using the frequencies for the normal modes for the gas is 7.22 which is in excellent agreement. For the *trans* conformer frequencies from the solid state had to be used. For the A′ block the theoretical tau value is 2.86 with the experimental value of 2.57 which is too low but the discrepancy is probably due to the association in the solid state. For the A″ block the theoretical value is 2.58 and the experimental value is 2.53 which is in excellent agreement. Therefore, Teller–Redlich calculations support the vibrational assignment for the Si-d_2 isotopomer.

The changes in the relative stabilities of the two conformers in going from the fluid states to the crystalline solid is probably due to two factors. The permanent dipole for the *trans* is predicted to be 40% larger than that of the *gauche* conformer. Therefore, in the liquid state which is a polar medium of the *trans* conformer stability will be increased compared to that of the *gauche* conformer. This is probably the reason why the energy difference for the two conformers was found to be nearly zero in the earlier vibrational study [7]. This effect can also assist along with the packing factor to the *trans* conformer being the stable rotamer in the solid. Similar results were also found [1] for the 1-chloropropane molecule where the stable conformer in the fluid states is the *gauche* rotamer but in the solid state the *trans* conformer is the stable form. Thus, the longer C–Si bond compared to the C–C bond does not appreciably effect the conformational behavior of chloromethyl methyl silane compared to that of the corresponding carbon analogue.

The normal vibrations are relatively pure modes for the *trans* conformer with significant mixing of the SiH_2 wag with the CH_3 rock and the two low frequency bends, SiCCl and CSiC in the A′ species. In the A″ species the CH_2 twist is significantly mixed with the SiH_2 twist whereas the remaining modes are relatively pure. For the *gauche* conformer the mixing is quite extensive with the modes indicated as the CH_3 rock and the SiC_3 stretch having less than 20% being contributed by these vibrations. Several of the other modes such as the CSiC bend, CH_3 torsion and the SiH_2 twist also have significant mixing. Thus, the descriptions provided for the vibrations of the *gauche* conformer are more for bookkeeping than to describe the atom motions involved.

Table 8
Observed and calculated (cm^{-1}) torsional transitions for chloromethyl methyl silane

Transition	Obs.	Calc.[a]	Δ
gauche			
$1 \mp \leftarrow 0 \pm$	87.0	87.3	0.3
$2 \pm \leftarrow 1 \mp$	85.0	85.0	0.0
trans			
$1 \leftarrow 0$	80.0	79.7	−0.3
$2 \leftarrow 1$	78.0	77.4	−0.6

[a]Values from potential parameters listed in Table 9.

We determined the potential parameters from the frequencies of the torsional transitions (Table 8) for the two conformers along with the enthalpy value from the xenon solution and the dihedral angle predicted for the *gauche* conformer from the MP2/6-31G* calculation. With these data, the potential function governing the internal rotation of this molecule has been calculated. The torsional potential is represented by a Fourier cosine series in the internal rotation angle, θ

$$V(\theta) = \sum_{i=1}^{6} \left(\frac{V_i}{2}\right)(1-\cos i\theta)$$

where θ and i are the torsional angle and foldness of the barrier, respectively. It was assumed that V_4 through V_6 were relatively small and they were not included in the series. The potential coefficients, V_1, V_2 and V_3 are calculated from the input of the torsional transition frequencies ΔH value, *gauche* dihedral angle and the internal rotation constants $F(\theta)$. The internal rotation constant varies as a function of the internal rotation angle, and this is approximated by another Fourier series

$$F(\phi) = F_0 + \sum_{i=1}^{6} F_i \cos i$$

The relaxation of the structural parameters, $B(\phi)$, during the internal rotation can be incorporated into the above equation by assuming them to be small periodic functions of the torsional angle of the general type

$$B(\phi) - a + b\cos\phi + c\sin\phi$$

Table 9
Potential energy coefficient (cm^{-1}) of chloromethyl methyl silane for the conformer interconversion

Coefficient	Value[a]	RHF/6–31G*
V_1	−202 ± 16	−110
V_2	−43 ± 16	−38
V_3	856 ± 5	778
V_6	–	18
ΔH	180 ± 37	126
Dihedral angle	120.7	118.5
trans/gauche barrier	775	714
gauche/gauche barrier	838	771
gauche/trans barrier	959	840

[a]Calculated using $F_0 = 1.011811$, $F_1 = -0.183056$, $F_2 = 0.112370$, $F_3 = -0.028214$, $F_4 = 0.010795$, $F_5 = -0.003130$, $F_6 = 0.001124$.

The series approximating the internal rotation constants for chloromethyl methyl silane was determined by using structural parameters from the MP2/6-31G* ab initio calculations. In the initial calculation of the potential function the transitions assigned as the $1 \leftarrow 0$ for the *trans* conformer, the $1 \pm \leftarrow 0^{-}_{+}$ for the *gauche* conformer, the enthalpy value of 180 cm^{-1}, and the dihedral angle of 120.3° was used to obtain the V_1, V_2 and V_3 terms. One additional transition for each conformer was added and the final results are given in Table 9. The determined parameters were then compared to those obtained from the RHF/6-31G* calculation (Table 9). The *trans* to *gauche* and *gauche* to *gauche* barriers have values of 775 and 838 cm^{-1}, respectively, from the far infrared and enthalpy data and the corresponding ab initio values are 714 and 771 cm^{-1}, respectively, which is in excellent agreement (Fig. 14).

The enthalpy value from the xenon solution has a very small statistical uncertainty which, of course, does not take into account problems associated with combination or overtone bands having frequencies near or almost identical to the bands being used for the determination. Possible interference from overtone bands is reduced by using the lower frequency fundamentals. Nevertheless, there is still problems associated with overlapping bands (Fig. 15) although the 738 cm^{-1} band used for one of the determinations

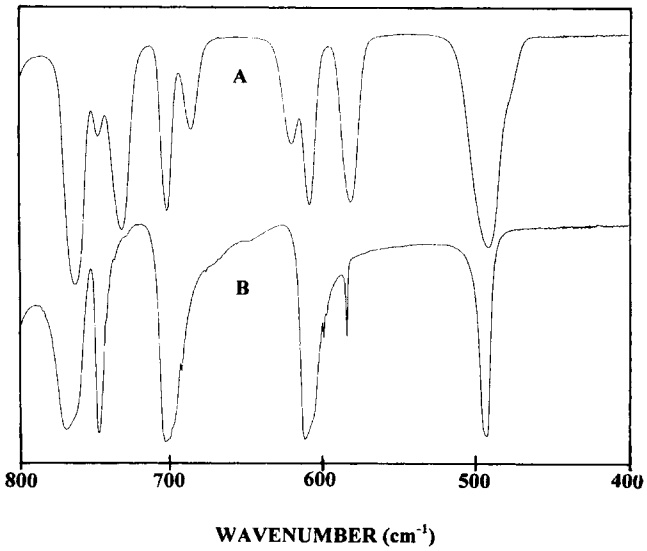

Fig. 15. Mid-infrared spectra range (800–400 cm^{-1}) of chloromethyl methyl silane-d_0: (A) unannealed solid; and (B) annealed solid.

seems to disappear completely from the spectrum of the annealed solid. Since the 584 cm^{-1} band is mainly due to the *gauche* conformer, we used this band with the 700 cm^{-1} to obtain a third value for the enthalpy difference. This pair of bands gave a value of 122 ± 13 cm^{-1}, which is the expected range since the 584 cm^{-1} band contains some absorption due to the *trans* conformer. Therefore, we believe the value obtained from only the two pairs of bands is a good value but the uncertainty should be more like 10% rather than the small statistical uncertainty of 2%, i.e. 180 ± 18 cm^{-1}. This value is in good agreement with the predicted value of 221 cm^{-1} obtained with the large basis set, i.e. MP2/6-311+G** (Table 4).

Utilizing the isolated Si–H stretching frequencies from the $ClCH_2SiHDCH_3$ isotopomer it is possible to calculate the Si–H distances (r_0) for the *gauche* conformer [17]. Utilizing the frequencies of 2174 and 2148 cm^{-1} for the two different Si–H vibrations for the *gauche* conformer the Si–H bond distances are calculated to be 1.482 and 1.487 Å. These values compare very well with the 1.485 and 1.490 Å predicted for these bond distances from the MP2/6-31G* calculations. The predicted Si–H bond distances from the MP2/6-311+G** calculations are shorter with values of 1.477 and 1.481 Å, respectively, which makes them smaller by 0.005 and 0.006 Å than the r_0 values obtained from the infrared spectrum. Therefore, the agreement from the MP2/6-31G* calculation is quite good and indicates that the structural parameters obtained from the relatively small 6-31G* basis set with electron correlation at the MP2 level provides good predictions of the structural parameters for these types of molecules.

As pointed out earlier, 1-chloropropane also has the *gauche* conformer as the stable rotamer in the fluid phase but in the solid the *trans* conformer is the stable form. Thus the longer C–Si bond compared to the corresponding C–C bond does not alter this change. Since an accurate determination of the experimental enthalpy for the conformational change in 1-chloropropane has not been made, a temperature study of the infrared spectra of a sample dissolved in xenon or other rare gases would be valuable for comparison with the current studies. Similar studies of 1-bromopropane would also be of interest since it is not known which conformer is the more stable form in the fluid phases.

Acknowledgements

JRD acknowledges the University of Missouri—Kansas City Trustees for a Faculty Fellowship award for partial financial support of this research.

References

[1] J.R. Durig, S.E. Godbey, J.F. Sullivan, J. Chem. Phys. 80 (1984) 5983.
[2] K. Yamanouchi, S. Yamamoto, M. Nakata, T. Fukuyama, H. Takeo, C. Matsumura and K. Kuchitsu, Ninth Austin Symposium on Molecular Structure, Austin, TX, 1982, Abstract No. A23.
[3] Y. Ogawa, S. Imazeki, H. Yamaguchi, H. Matsuura, Bull. Chem. Soc. Jpn. 51 (1978) 748.
[4] C. Komaki, I. Ichishima, K. Kuratani, T. Miyazawa, T. Shimanouchi, S. Mizushima, Bull. Chem. Soc. Jpn. 28 (1955) 330.
[5] E. Hirota, J. Chem. Phys. 37 (1962) 283.
[6] G.A. Crowder, H.K. Mao, J. Mol. Struct. 18 (1973) 33.
[7] M. Hayaski, K. Ohno, H. Murata, Bull. Chem. Soc. Jpn. 46 (1973) 797.
[8] F.A. Miller, B.M. Harney, Appl. Spectrosc. 24 (1970) 291.
[9] W.A. Herrebout, B.J. van der Veken, Wang Aiyang, J.R. Durig, J. Phys. Chem. 99 (1995) 578.
[10] W.A. Herrebout, B.J. van der Veken, J. Phys. Chem. 100 (1996) 9671.
[11] Gaussian 92/DFT, M.J. Frisch, G.W. Trucks, M. Head-Gordon, P.M.W. Gill, M.W. Wong, J.B. Foresman, B.G. Johnson, H.B. Schlegel, M.A. Robb, E.S. Replogle, R. Gomperts, J.L. Andres, K. Raghavachari, J.S. Binkley, C. Gonzalez, R.L. Martin, D.J. Fox, D.J. Defrees, J. Baker, J.J.P. Stewart, and J.A. Pople, Gaussian 92/DFT, Gaussian Inc., Pittsburgh PA, 1992.
[12] P. Pulay, Mol. Phys. 17 (1969) 197.
[13] T.A. Mohamed, H.D. Stidham, A.G. Gamil, M.S. Afifi, J.R. Durig, J. Mol. Struct. 299 (1993) 111.
[14] R.V. Belyakov, V.Z. Szvgorodzii, V.S. Mastryukov, Zh. Strukt. Khim. 30 (1989) 27.
[15] J.H. Schachtschneider, Vibrational Analysis of Polyatomic Molecules, Parts V and VI, Technical Report Nos. 231 and 57, Shell Development Co., Houston TX, 1964 and 1965.
[16] G.W. Chantry, in: A. Anderson (Ed.) *The Raman Effect*, Vol. 1, Chap. 2, Marcel Dekker, New York, 1971.
[17] J.L. Duncan, J.L. Harvie, D.C. McKean, S. Cradock, J. Mol. Struct. 145 (1986) 225.